*International Journal on Algae, 2022, 24(4): 383–398*

# Synthesis and Characterization of Biofilm from Microalgae Residue

**Wong Y.C.* & Heera M.**

*Advance Industrial Biotechnology Cluster (AdBiC), Faculty of Bioengineering and Technology, University Malaysia Kelantan, Jeli Campus, Jeli 17600, Kelantan, Malaysia*

*yeeching@umk.edu.my

Received: 23 May 2022/Accepted 17 June 2022/Published on line 29 December 2022

**ABSTRACT**: Bioplastic manufacture requires a chemical process to convert organic material to plastic, which results in high production costs. This lead to the invention of biofilm, using microalgae which is a non-food-based raw material, as a substitute for plastics. Biofilms, using microalgae, are beneficial for the environment, waste, and cost-effective scalable production. The microalgal species identified in the study are *Tribonema* sp., *Closterium* sp., *Trachelomonas* sp., and *Chlorella* sp. Six tests were undertaken on the biofilm: Gas Chromatography-Mass Spectrometry (GCMS), Fourier-transform infrared (FTIR) analysis, Thermogravimetric Analysis (TGA), film moisture content, water absorption, and biodegradation testing. Based on the result following characterization of GCMS, the presence of Acetamide (92.45%), Silanediol, dimethyl (87.69%), and 4-Ethylbenzoic acid, cyclohexyl ester (73.15%) compound was analyzed in microalgal culture. The main functional groups obtained from FTIR were O-H, C-H, and C=C. Additionally, Biofilm S (2.98%) has greater thermal stability than biofilm M1 (1.00%) and M2 (0.24%) at the highest temperature. Meanwhile, biofilm (100% microalgae residue) has a low moisture content (7.69%), low moisture absorption (150.00%), and a high biodegradable rate (74%). Generally, low moisture content and moisture absorption could make the biofilm lighter in weight, enhance its shelf life, and provide adequate flexibility. It also improves waste management of conventional plastics, which can decompose in a short amount of time. This study has shown that the amount of microalgae residue in the formulation significantly affects the appearance, chemical, physical and biodegradable properties of the biofilm.

**KEY WORDS**: microalgae; residue; biofilm; algae cultivation; glycerol

ISSN 1521-9429

## INTRODUCTION

Plastics are produced for a wide range of consumer and industrial applications. Plastics are widely used due to their favourable characteristics making them an extremely versatile, relatively low density, low-cost, and excellent thermal and electrical insulator. They can be easily molded into complex shapes, making them ideal for a wide range of functions.

Microalgae are typically unicellular microorganisms with the ability to aggregate, allowing them to form various cell structures such as colonial, filamentous, and unicellular (Palma et al., 2017). The term "algal biofilms" therefore refers to microalgae-dominated biofilm communities that colonize illuminated surfaces in the presence of moisture and nutrients. Hence, microalgae are used as alternative biomass to produce biofilm, which can serve as an excellent plastic substitute, owing to its many advantages such as high yield, cost-effective scalable production, and reduced waste (Fabra et al., 2017).

For this study, microalgae biolfim was characterized using several tests such as Gas Chromatography-Mass Spectrometry (GC-MS), Fourier-transform infrared spectroscopy (FTIR), Thermogravimetric Analysis (TGA), film moisture content, water absorption, and biodegradation test. Moreover, this study was undertaken by synthesizing microalgae biofilm from microalgae residue at different residue percentages (0%, 5%, 25%, 50%, 75%, and 100%) under optimum growth conditions. Hence, the chemical, physical and biodegradable properties were analyzed using the tests mentioned above.

## MATERIALS AND METHODS

### Identification of microalgae (in the fish pond)

10 mL of a water sample from the UMK fishpond was collected and stored inside a sample bottle irrespective of identification purpose. Using a compound microscope, microalgae species were identified.

### Cultivation of microalgae

The cultivation steps began with, 2 L of a microalgal sample poured into a plastic aquarium. Then 4 L of distilled water and 12 L of tap water were sunsequently added to the aquarium. Followed by 35 g of grounded NPK fertilizer at a ratio of 12 : 12 : 17 of nitrogen, phosphorus, and potassium also added into the aquarium. The culture was maintained at an optimum pH (pH 6–8) and temperature (25–35 $^{o}$C). The aquarium was covered with aluminium foil and kept under a fluorescent light. The aquarium was monitored steadily for a 7 days period. The microalgal–cell density was counted using a spectrophotometer for a 7 days period (Ra, 2020).

**Centrifugation**

The cultured microalgae was centrifuged at 18–20 $^{o}$C at a speed of 10,000 x rpm for 15 min until it formed a microalgal paste. It was then washed twice with distilled water before the drying process. The microalgal paste was oven-dried overnight at 60 $^{o}$C (for 12–18 hours) until it reached a constant weight. The dried residue was stored in Ziploc bags and kept in a desiccator. The desiccator is used to preserve the microalgae residue (Wong, Shahirah, 2019).

**Preparation of biofilm**

The experiment began with 2 g of starch powder dispersed in a beaker containing distilled water. It was then gently stirred at 90 $^{o}$C for 30 min to induce starch gelatinization. The mixture consists of starch: vinegar: and glycerol based on the ratio of 2 : 1 : 1. Meanwhile, 0.05 g of microalgal residue were treated with 10 mL distilled water to obtain 5% microalgal residue and subsequently incorporated into the mixture prior to the gelatinization step. The solution was heated until it coagulated. Once the mixture became thick, 30 mL of the 5% microalgae residue solution was poured into a petri dish. These steps were repeated according to the demand of microalgal residue (0 g, 0.25 g, 0.5 g, 0.75 g, and 1 g) which was treated with 100 mL distilled water to obtain 0%, 25%, 50%, 75%, and 100% of microalgae residue respectively. The petri dish was labelled and transferred to the oven for 1 hour at 60 $^{o}$C for the drying process of the film (Sumarni et al., 2017).

**Analysis using GC-MS**

1 mL of the microalgae culture sample was inoculated through the machine. The column of the machine utilized was DB%-MS UI with a measurement of 30 × 0.25 × 0.25 mm size. The detector and injector temperatures were set at 280 $^{o}$C and 200 $^{o}$C respectively. The initial oven ramping was started at 40 $^{o}$C for 2 min and then gradually increased to 280 $^{o}$C at the rate of 10 min$^{-1}$ with 5 min of hold time. The duration was set for 29 min. The carrier gas was helium, which was pumped at a 1.2 mL/min rate. Electron Impact (EI) spectra in the m/z 40 to 600 mass range were obtained in full scans at 70 eV. The retention period for peak detection was obtained and displayed in a graph (Wong, Shahirah, 2019).

**Analysis using FTIR**

Small samples of film were cut into pieces measuring 3 × 2 cm$^2$ and placed on ATR crystal to cover the crystal's surface. The wavelength range which was used for this analysis is between 450 cm$^{-1}$ and 4000 cm$^{-1}$ at room temperature. For the sample to be in contact with the ATR crystal, the screw was tightened. The angle of the incidence of the

crystal wasset to 45º. The graph was digitally displayed representing the sample content (Luís et al., 2019).

**Analysis using TGA**

The sample (4 × 4 mm) was sliced and placed in an aluminium crucible, which was then heated to 500 °C from 30 °C at a rate of 5 °C $min^{-1}$ in a nitrogen environment under a constant load of 100 mN. A sealed aluminium pan and an empty sealed pan were placed on the calorimeter. Under a nitrogen environment, the change in heat per gram of sample was measured using a computerized system at a constant temperature for 60 min (Hazrol et al., 2021).

**Analysis of film moisture**

The film sample was cut into 2 and 6 $cm^2$ pieces. The original weight of the film samples was measured using a digital measuring scale (*Wi*). The samples were weighed after drying for 24 hours at 105 °C (*Wf*). Equation 1 below was used to calculate the moisture content of each film sample.

$$\text{Moisture content (\%)} = (Wi - Wf) / Wi \times 100 \quad (1).$$

**Analysis of water absorption**

Film samples measuring 2 × 6 $cm^2$ were cut and dried for 3 hours at 105 °C in a laboratory oven, then cooled and weighed straight away (*Mi*). At room temperature, the selected sample was submerged in distilled water (100 mL). After a specific amount of time in the water, the sample was removed, wiped with a cloth, and reweighed ($M_f$). Equation 2 below was used to calculate the water absorption of each film sample

$$\text{Water absorption (\%)} = (M_f - M_i) / M_i \times 100 \quad (2).$$

**Analysis of biodegradability**

The film sample was cut into 2 × 6 $cm^2$ pieces. The initial weight ($m_0$) of the film was measured, labelled, and recorded. Then, the sample was buried in soil at a depth of 10 cm for 14 days. After the 14$^{th}$ day, the sample was collected and washed twice using distilled water. Following which it was oven-dried at 60 $^{o}$C until it reached a constant weight, and the final weight ($m_t$) of films was recorded. The percentage of weight loss (*WL*, %) during the degradation process was calculated using equation 3 shown below (Carissimi et al., 2018).

$$WL(\%) = \frac{m_0 - m_t}{m_0} \times 100 \quad (3).$$

## RESULTS AND DISCUSSION

### Identification of microalgae species

A mixture of microalgae species was found and identified in the sample using a compound microscope with 10x magnification. The microalgae species identified in the sample were *Tribonema* sp., *Closterium* sp., *Trachelomonas* sp., and *Chlorella* sp. as shown in Fig. 1.

### Cultivation of microalgae

According to the findings in Fig. 2, *a*, the microalgae growth rate in the aquarium was increasing, indicating a high production of microalgae biomass when compared to earlier studies. This may be a product of growing microalgae in a closed environment where it is possible to reduce contamination risks and increase productivity due to the high photosynthetic rate (Chia et al., 2020). Besides that, continuous effective stirring using an aerator–maintains cells in suspension, distributes nutrients, increases gas exchange, and eliminated thermal separation (Wang, Lan, 2018).

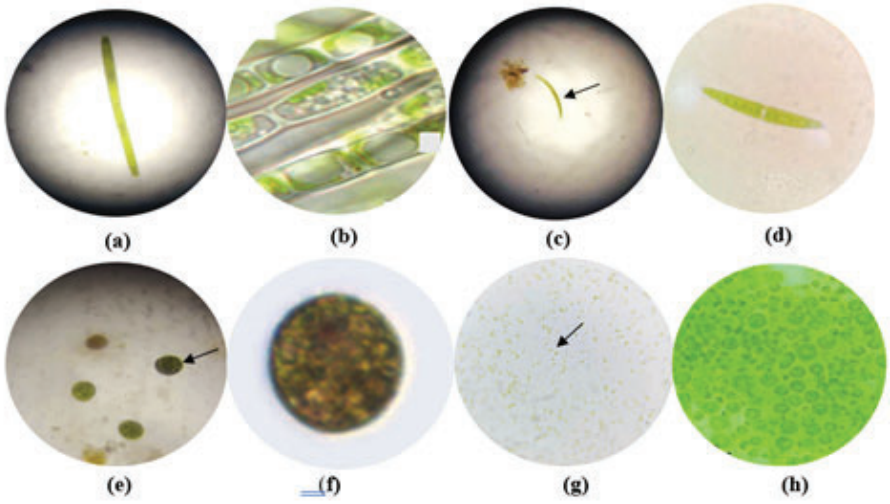


**FIG. 1**: *a* – *Tribonema* sp.; *b* – Wang et al., 2017; *c* – *Closterium* sp.; *d* – Nuttapong Saetang, Sawitree Tipnee, 2021; *e* – *Trachelomonas* sp.; *f* – Žerdoner Čalasan et al., 2020; *g* – *Chlorella* sp.; *h* – Bhuyar et al., 2020

Based on Fig. 2, *b*, the pH range of microalgae growth is between pH 3.65 to pH 5.3. This could be due to the initial pH value of tap water or the $CO_2$ presence in the water. According to Dolganyuk (2020), increased $CO_2$ availability in the aqueous phase can boost

biomass production in microalgae cultures, conversely, a fall in pH due to increased $CO_2$ availability in the aqueous phase can stifle the growth of certain species of microalgae (Dolganyuk et al., 2020).

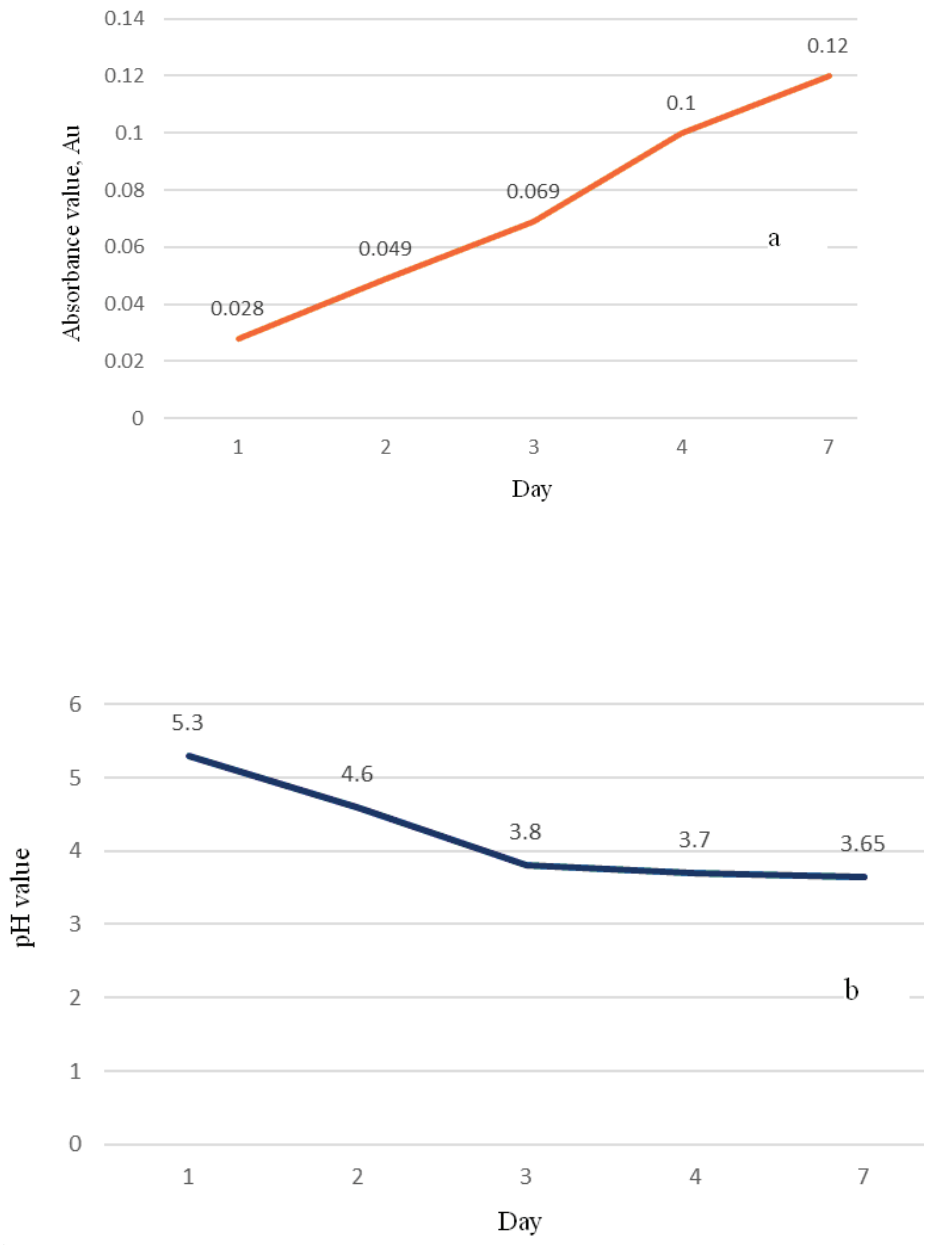


**FIG. 2**: *a* – growth of microalgae culture; *b* – pH of microalgae culture

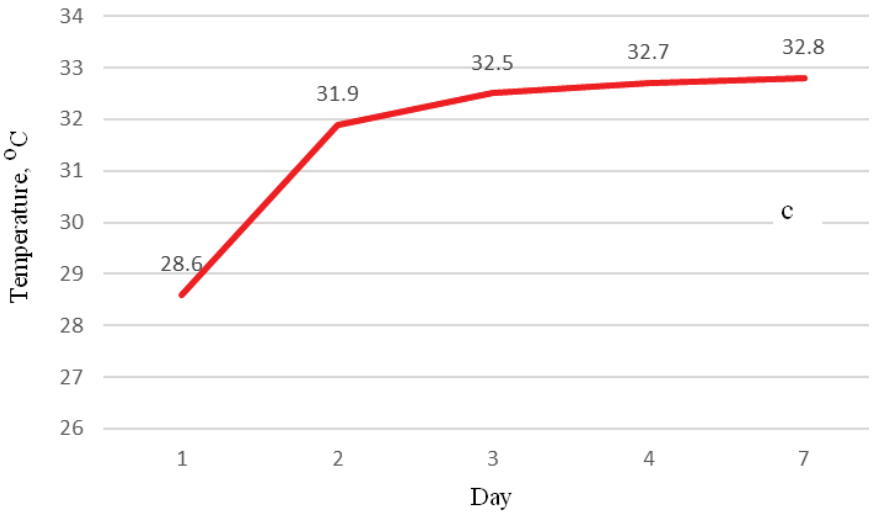


**FIG. 2**: *c* – the temperature of microalgae culture

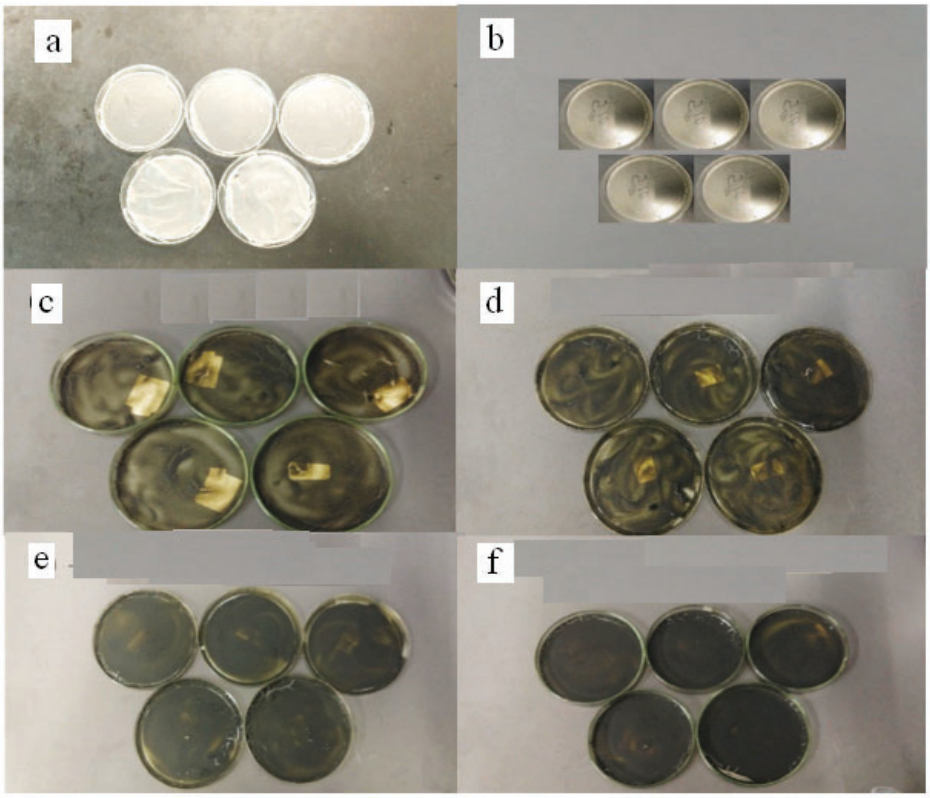


**FIG. 3**: Microalgae biofilms with 0% (*a*); 5% (*b*); 25% (*c*); 50% (*d*); 75% (*e*); 100% (*f*) concentrations

Microalgae thrive best at temperatures between 27 $^{o}$C and 30 $^{o}$C. At 32.8 °C, the greatest absorbance reading was obtained which is 0.12 Au as shown in Fig. 2, *c*. This does not comply with reports by Dolganyuk et al. (2020), where an increase in cultivation temperature lead to a biomass yield decrease (Dolganyuk et al., 2020). This might be due to the microalgae strains found in the pond having high resistance at high temperatures. Additionally, the transition from the exponential to the stationary phase may cause Fatty Acid (FA) saturation and polyunsaturated FA levels to be present in the STA phase, whereas algal cells generally show an increase in saturated FAs (Aziz et al., 2020).

**Preparation of biofilm**

Based on the result obtained in Fig. 3, the obvious change that can be observed in Fig. 3 was the color intensity. As the concentration ratio increased from 0% to 100%, the color of microalgal biofilms turned from clear to dark green in color. The microalgal biofilms that form are a thin layer, which is flexible, light and slightly stretchable.

**Gas chromatography-mass spectrometry (GC-MS)**

The peaks received were identified based on library research or the National Institute of Standard and Technology (NIST) database. The peak at the retention time of 5.488–5.531 min is named Acetamide with a 30.35% area, the second significant peak is at the retention time of 5.178–5.226 min named Silanediol, dimethyl- with 21.82% area and the third, significantly less prominent peak is at the retention time of 7.024 to 7.665 min named 4-Ethylbenzoic acid, cyclohexyl ester with 1.94% area which can be seen in Table 1.

**TABLE 1**: Compounds contained in microalgae biomass

| Compound name | Score | Formula | Peak, # | Area, % |
|---|---|---|---|---|
| Acetamide | 92.45 | $C_2H_5NO$ | 7 | 30.35 |
| Silanediol, dimethyl- | 87.69 | $C_2H_8O_2Si$ | 6 | 21.82 |
| 4-Ethylbenzoic acid, cyclohexyl ester | 73.15 | $C_{15}H_{20}O_2$ | 10 | 1.94 |

**Fourier transform infrared spectroscopy (FTIR) analysis**

The FTIR spectra of the microalgal biomass represents the alcohol group (OH), carboxyl group (COOH), amino ($NH_2$), and other groups associated with an organic compound. Referred to as biofilm M1 and M2 analysis, the band at 3276.66 cm$^{-1}$ and 3247.35 cm$^{-1}$ respectively indicates the existence of an O-H bond, meanwhile, the band at

1646.92 and 1646.93 respectively are equivalent to C=C indicating the presence of cyclic alkene. The presence of the C=C and O-H bond is related to the polysaccharide presence in microalgae residue (Johnsson, Steuer, 2018). In addition, the peak in the high-intensity region 3550–3200 $cm^{-1}$ indicates the presence of lipids in biomass, suggesting a lipid peak in this region due to symmetrical and asymmetrical stretching vibration of $CH_2$ (Arif et al., 2021). The C, H, and O elements were detected in all the compounds found in the GCMS analysis. As a result, the existence of O-H, C=C, and C-H in the analysis was expected.

Based on biofilm S, the band 3274.18 $cm^{-1}$ shows the existence of an O-H stretch bond respectively at the end of the polymer chain of starch and plasticizer, while the band identified at 2930.34 $cm^{-1}$ indicates C-H stretching. The C-H molecules start to vibrate, causing H atoms to separate from C (Hazrol et al., 2021). The peak of 1418.33 $cm^{-1}$ was assigned to the bending mode of the absorbed water O-H, and the peak around 1077.62 $cm^{-1}$ was attributed to C-O bonding. The identifiable bands were found at 1716.54 and attributed to C=O, and 1646.91 was attributed to N-H bands forming intermolecular hydrogen bonds with the O-H of a glycerol compound. Thus, the film gains significant numbers of O-H groups in their matrices that can increase hydrogen bond and attract moisture, see Table 2 (Nor et al., 2017).

**TABLE 2**: Classification of functional group and bond type in respective wave number

| Wavenumber, $cm^{-1}$ | Type of bond | Functional groupe |
|---|---|---|
| 3550–3200 | O-H | Alcohol |
| 3300–2500 | O-H | Carboxylic acid |
| 3000–2840 | C-H | Alkene |
| 1720–1706 | C=O | Carboxylic acid |
| 1658–1648 | C=C | Alkene |
| 1650–1580 | N-H | Amine |
| 1650–1566 | C=C | Cyclic alkene |
| 1420–1330 | O-H | Alcohol |
| 1250–1020 | C-N | Amine |
| 1085–1050 | C-O | Primary alcohol |
| 1075–1020 | C-O | Ether |

**TABLE 3**: TGA analysis of biofilm

| Biofilm | Temperature range, $^0$C | Weight loss, % | Residual weight, % |
|---|---|---|---|
| S | 37–85 | 16.62 | 83.32 |
| | 85–228 | 29.68 | 53.63 |
| | 228–496 | 50.65 | 2.98 |
| M1 | 34–88 | 18.82 | 81.13 |
| | 88–234 | 65.62 | 15.51 |
| | 234–493 | 16.51 | 1.0 |
| M2 | 36–93 | 34.02 | 65.91 |
| | 93–238 | 55.97 | 9.94 |
| | 238–498 | 9.70 | 0.24 |

Based on the results, biofilm M1 and M2 contributed to a higher percentage of weight loss (65.62% and 55.97%) respectively. The highest percentage weight loss of M1 and M2 happen due to thermal decomposition of components that made up the biofilm, which is a benefit of microalgae (Table 3). Combustion of microalgae organic material such as carbohydrates, protein and lipid happen in this phase which is why this stage is also known as the active pyrolytic zone. This context is supported with the observation that Stage E and H of the DTG curve in M1 and M2. The curve shows a steep decrease which denoted the active combustion reactions zones (Khoo et al., 2020).

On the other hand, at the third distinctive step of biofilm M1 and M2, the weight loss rate is slightly lower, 16.51% and 9.70% respectively. This indicates that most of the components in the biofilm decomposed within a reasonable range of time, and degradation of carbonaceous substance is retained in solid residue. Stage F and I of the DTG curve in M1 and M2 also show small peaks which indicates that, less biofilm weight loss is observed at this stage. The decomposition step may be attributed to the decomposition of minerals or inorganic material, which were found in high ash content with good agreement. The biofilm S shows highest weight loss at the third step (50.65%), and Stage C shows highest steep. This phenomenon may be attributed to the thermal decomposition of components that made up the biofilm. Despite the majority of weight loss occuring at this stage, for the biofilm S, a high level of residue remains.

**Film moisture content test**

Based on Fig. 4 the film containing 100% microalgae biomass shows the lowest moisture content (7.69%), compared to other films containing microalgae biomass. This

might be due to higher concentration of hydrophobic compounds such as hydrocarbons in the microalgae biomass. The formation of intermolecular hydrogen bonds between the polymeric matrix and the incorporated microalgae biomass, can be attributed to the formation of a crosslinked network structure; this may decrease the free volume of the polymeric matrix, resulting in a decrease in the diffusion rate of water vapour molecules through the biofilm (Deshmukh et al., 2021). Additionally, a higher lipid concentration in microalgae biomass films may be attributed to its low moisture content, considering it decreases water-starch interactions due to their hydrophobic characteristics (Carissimi et al., 2018).

Meanwhile, when 100% microalgae film is compared with the control, 0% microalgae, the moisture value is higher (84.15%). According to Hazrol et al. (2021), the hydroxyl groups in glycerol have a strong affinity to water molecules; enabling glycerol-containing films to easily retain water within their matrix and form hydrogen bonds (Hazrol et al., 2021). In addition, films with high moisture content also have greater flexibility. Hence, glycerol acted as a water-holding agent which results in a high moisture content film containing a 0% concentration of microalgae biomass.

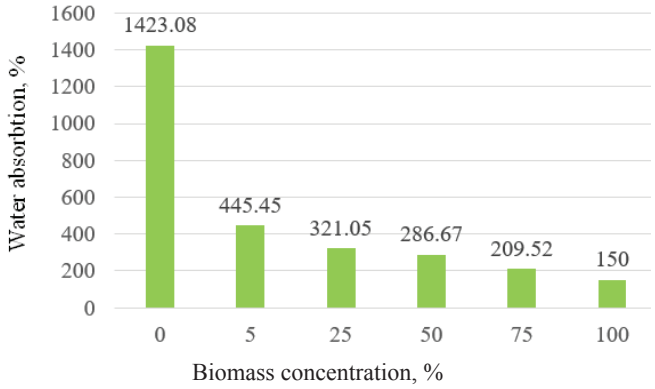


**FIG. 4**: The water absorption of biofilm with different concentrations biomass

**Water absorption test**

Based on Fig. 5, film made of 100% microalgae biomass shows the lowest absorption rate (150%) compared to other films containing microalgae. From visual observation of the 100% microalgae biomass, the film dissolved less, even after 1 hour of immersion, in distilled water. This can be attributed to the addition of microalgae biomass, increasing the surface sensitivity to water, but decreasing the overall water absorption kinetics in the selected timeframe (Cinar et al., 2020). Studies have shown that the addition of microalgae biomass (30 php) lowers the water contact angle from 41° to 22° in the sample plasticized

with glycerol (Ciapponi et al., 2019). Furthermore, regardless of the nature of the biomass employed, the loss of soluble material indicated a lower fall in value of plasticizer content. This is consistent with the observation that glycerol loss tends to increase during immersion (López Rocha et al., 2020). Thus, as the concentration of microalgae biomass in the film formulation increases, the water absorption of the film decreases.

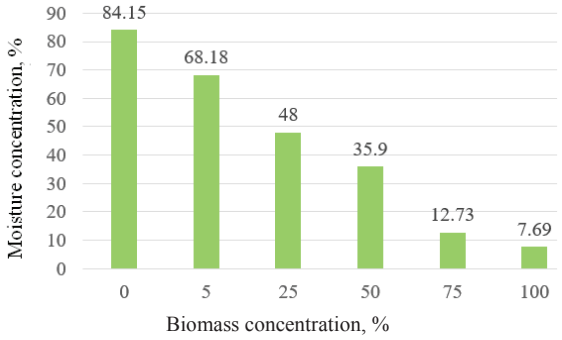


**FIG. 5**: The moisture content of biofilm with different concentration biomass

On the other hand, starch films become heavier compared to the initial weight before immersing it into water. Water absorption is important because water works as a plasticizer. Plasticized films at higher plasticizer and moisture content had greater flexibility. For 0% microalgae film, the water absorption of film was high (1423.08%) because the creation of hydrogen bonds with starch produced by the presence of hydroxyl groups inside the plasticizer molecules causes a stronger tendency for water absorption into plasticized polymers. Besides that, due to hygroscopic properties, starch chains have a great inclination to form intermolecular interactions, which functions to lose or gain water to achieve equilibrium with ambient water. Hence it makes starch films more brittle and rapidly or highly soluble in water, thus limiting its application (Othman et al., 2019).

**Biodegradation test**

As clearly shown in Fig. 6, the percentage biodegradation of biofilm increases as the concentration of microalgae increases in the preparation of biofilm. 100% microalgae biomass in biofilm shows the highest rate of biodegradation at 74%, whilst the 0% concentration of microalgae biomass in biofilm only shows 20% degradation. This is thought to be due to the synthesis of ligninolytic and exopolysaccharide enzymes by algae adhering to the surface, which will start the biodegradation process essential to the biodegradation of biofilms (Chia et al., 2020). Moreover, microalgae biomass is also known to have a plentiful supply of biomolecules, such as polysaccharides, amino acids, vitamins and many more. For instance, *Spirulina platensis* species microalgae have

phycobiliproteins, which hold functional properties including antimicrobial, anti-inflammatory and antioxidant activity. As a result, microalgae could be a promising alternative for the manufacturing of biodegradable materials, which are both sustainable and affordable (Moghaddas Kia et al., 2018). When compared to the control sample, 0% microalgae biomass, degradation is lower compared to the films that contain microalgae. This indicates that the addition of microalgae biomass enhances the degradability of the film in the soil by microorganism.

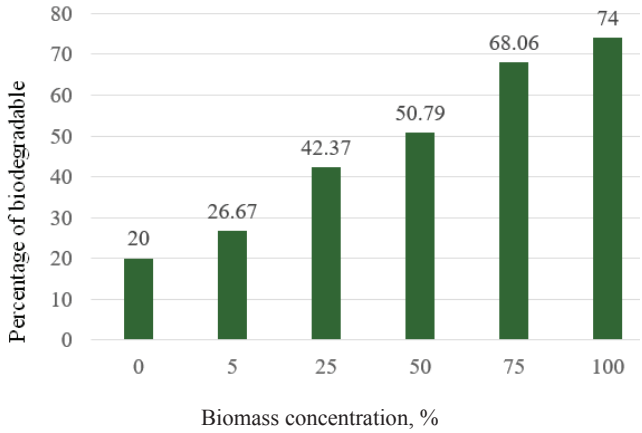


**FIG. 6**: The percentage of biodegradable of biofilm with different concentration biomass

The rate of degradation-at 0% is low, which may be due to the short period of time the experiment was conducted in. The starch-based biofilm takes at least 3 to 6 months to break down into small pieces and fully decompose. Thus, this could be one of the reasons why the rate of degradation is low when the biofilm contains no microalgae biomass, which would increase the speed of the degradation process.

## CONCLUSIONS

In this study, microalgae biomass was obtained using a cultivation process, and further used in biofilm production. Chemical and physical properties of the synthesized biofilm were analysed using several related tests. From GCMS analysis, it shows C, H and O elements were detected in all the compounds from the culture, which further proves the existence of O-H, C=C and C-H in the analysis of FTIR. Biofilm M1(50%) and biofilm M2 (100%) contributed to a lower ignition and higher burn out, producing a residual weight of 1.00% and 024% respectively, compared to biofilm S (0%) which was found to be 2.98% at the highest temperature. Therefore, biofilm M1 and M2 have a lower thermal stability compared to biofilm S1. Furthermore, a low moisture content (7.69%) and water absorption

(150.00%) in 100% microalgae biofilm will help to avoid the promotion of oxidation which leads to contamination. The formulation of microalgae biofilm also indicates that the higher the microalgae residue in the film (100% biofilm), the better the degradation (74.00%) of biofilm within a reasonable time frame, without causing damage. Hence, according to the aforementioned characterization in this study, there is still a need for more research development of biofilm production processes using microalgae to overcome the economic feasibility problems in industrial-scale implementations. Thus, preventing the wider usage of plastic or bioplastic products in the market and reduce global environmental damage through appropriate decomposition.

**ACKNOWLEDGMENTS**

The authors express their sincere appreciation to UMK Prototype Research Grant (UMK-PRO) R/PRO/A1300/00457A/004/2020/00756 and the Advance Industrial Biotechnology Cluster (AdBiC), Faculty of Bioengineering and Technology, University Malaysia Kelantan, Jeli Campus for the financial support and facilities which made this study possible.

**REFERENCES**

Arif M., Li Y., El-Dalatony M.M., Zhang C., Li X., Salama E.S. 2021. A complete characterization of microalgal biomass through FTIR/TGA/CHNS analysis: An approach for biofuel generation and nutrients removal. *Renew. Energy*. 163: 1973–1982. https://doi.org/10.1016/j.renene.2020.10.066

Aziz M.M.A., Kassim K.A., Shokravi Z., Jakarni F.M. Liu H., Zaini N., Tan L.S., Islam A.B.M.S., Shokravi H. 2020. Two-stage cultivation strategy for simultaneous increases in growth rate and lipid content of microalgae: A review. *Renew. Sustain. Energy Rev.* 119: 109621. https://doi.org/10.1016/j.rser.2019.109621

Bhuyar P., Yusoff M.M., Rahim M.H.A., Sundararaju S., Maniam G.P., Govindan N. 2020. Effect of plant hormones on the production of biomass and lipid extraction for biodiesel production from microalgae chlorella sp. *J. Microbiol. Biotechnol. Food Sci.* 9(4): 671–674. https://doi.org/10.15414/JMBFS.2020.9.4.671-674

Carissimi M., Flôres S.H., Rech R. 2018. Effect of microalgae addition on active biodegradable starch film. *Algal Res.* 32: 201–209. https://doi.org/10.1016/j.algal.2018.04.001

Chia W.Y., Ying Tang D.Y., Khoo K.S., Kay Lup A.N., Chew K.W. 2020. Nature's fight against plastic pollution: Algae for plastic biodegradation and bioplastics production. *Environ. Sci. Ecotechnol.* 4: 100065. https://doi.org/10.1016/j.ese.2020.100065

Ciapponi R., Turri S., Levi M. 2019. Mechanical reinforcement by microalgal biofiller in novel thermoplastic biocompounds from plasticized gluten. *Materials* (Basel). 12(9): 1476. https://doi.org/10.3390/ma12091476

Cinar S.O., Chong Z.K., Kucuker M.A., Wieczorek N., Cengiz U., Kuchta K. 2020. Bioplastic production from microalgae: A review. *Int. J. Environ. Res. Publ. Health.* 17(11): 1–21. https://doi.org/10.3390/ijerph17113842

Deshmukh A.R., Aloui H., Khomlaem C., Neg A., Jin-HoYun, Beom Soo Kim. 2021. Biodegradable films based on chitosan and defatted *Chlorella* biomass: Functional and physical characterization. *Food Chem.* 337: 127777. https://doi.org/10.1016/j.foodchem.2020.127777

Dolganyuk V., Belova D., Babich O., Prosekov A. 2020. Microalgae: A promising source of valuable bioproducts. *Biomolecules*. 10(8): 1–24. https://doi.org/10.3390/biom10081153

Fabra M.J., Martínez-Sanz M., Gómez-Mascaraque L.G., Coll-Marqués J.M., Martínez J.C., López-Rubio A. 2017. Development and characterization of hybrid corn starch-microalgae films: Effect of ultrasound pre-treatment on structural, barrier and mechanical performance. *Algal Res.* 28: 80–87. https://doi.org/10.1016/j.algal.2017.10.010

Hazrol M.D., Sapuan S.M., Zainudin E.S., Zuhri M.Y.M. 2021. Corn Starch (Zea mays) Biopolymer Plastic Reaction in Combination with Sorbitol and Glycerol. *Polymers* (Basel). 13(2): 242.

Johnsson N., Steuer F. 2018. *Bioplastic material from microalgae Extraction of starch and PHA from microalgae to create a bioplastic material*. Stockholm: KTH Roy. Inst. Technol.

Khoo C.G., Lam M.K., Mohamed A.R., Lee K.T. 2020. Hydrochar production from high-ash low-lipid microalgal biomass via hydrothermal carbonization: Effects of operational parameters and product characterization. *Environ. Res.* 188: 109828. https://doi.org/10.1016/j.envres.2020.109828

López Rocha C.J., Álvarez-Castillo E., Estrada Yáñez M.R., Bengoechea C., Guerrero A., Orta Ledesma M.T. 2020. Development of bioplastics from a microalgae consortium from wastewater. *J. Environ. Manage.* 263: https://doi.org/10.1016/j.jenvman.2020.110353

Luís Â., Domingues F., Ramos A. 2019. Production of hydrophobic zein-based films bioinspired by the lotus leaf surface: characterization and bioactive properties. *Microorganisms*. 7(8): 267. https://doi.org/10.3390/microorganisms7080267

Moghaddas Kia E., Ghasempour Z., Alizadeh M. 2018. Fabrication of an eco-friendly antioxidant biocomposite: Zedo gum/sodium caseinate film by incorporating microalgae (*Spirulina platensis*). *J. Appl. Polym. Sci.* 135(13). https://doi.org/10.1002/app.46024

Nor M.H.M., Nazmi N.N.M., Sarbon N.M. 2017. Effects of plasticizer concentrations on functional properties of chicken skin gelatin films. *Int. Food Res. J.* 24(5): 1910–1918.

Nuttapong Saetang, Sawitree Tipnee. 2021. Towards a sustainable approach for the development of biodiesel microalgae, *Closterium* sp. *Maejo Int. J. Energ. Environ. Comm.* 3(1): 25–29. https://doi.org/10.54279/mijeec.v3i1.245114

Othman S.H., Kechik N.R.A., Shapi'i R.A., Talib R.A., Tawakkal I.S.M.A. 2019. Water sorption and mechanical properties of starch/chitosan nanoparticle films. *J. Nanomat.* https://doi.org/10.1155/2019/3843949

Palma H., Killoran E., Sheehan M., Berner F., Heimann K. 2017. Assessment of microalga biofilms for simultaneous remediation and biofuel generation in mine tailings water. *Biores. Technol.* 234: 327–335. https://doi.org/10.1016/j.biortech.2017.03.063

Sumarni W., Prasetya A.T., Rahayu E.F. 2017. Effect of Glycerol on Physical Properties of Biofilms Gembili Starch (Dioscorea Esculenta) – Chitosan. *Proc. Chem. Conf.* 2: 56–65. [Online]. Available: http://jos.unsoed.ac.id/index.php/jccp/article/view/1

Wang C., Lan C.Q. 2018. Effects of shear stress on microalgae – A review. *Biotechnol. Adv.* 36(4): 986–1002. https://doi.org/10.1016/j.biotechadv.2018.03.001

Wang H., Zhou W., Shao H., Liu T. 2017. A comparative analysis of biomass and lipid content in five *Tribonema* sp. strains at autotrophic, heterotrophic, and mixotrophic cultivation. *Algal Res.* 24: 284–289. https://doi.org/10.1016/j.algal.2017.04.020

Wong Y.C., Shahirah R. 2019. Effect of Different Solvent and Ratio Towards Microalgae Oil Production by Ultrasonic Assisted Soxhlet Extraction Techniques. *Orient. J. Chem.* 35(4): 1377–1383. https://doi.org/10.13005/ojc/350418

Žerdoner Čalasan A., Kretschmann J., Gottschling M. 2020. Contemporary integrative taxonomy for sexually deprived protists: A case study of *Trachelomonas* (*Euglenaceae*) from western Ukraine. *Taxon*. 69(1): 28–42. https://doi.org/10.1002/tax.12206